Physica A 428 (2015) 103–110

Contents lists available at ScienceDirect

Physica A

journal homepage: www.elsevier.com/locate/physa

Growing scale-free networks with tunable distributions of triad motifs

Shuguang Li [a,*], Jianping Yuan [b], Yong Shi [c], Juan Cristóbal Zagal [d]

[a] Sibley School of Mechanical and Aerospace Engineering, Cornell University, Ithaca, 14850 NY, USA
[b] School of Astronautics, Northwestern Polytechnical University, Xi'an, 710072 Shaanxi, China
[c] Schaefer School of Engineering and Science, Stevens Institute of Technology, Hoboken, 07030-5991 NJ, USA
[d] Department of Mechanical Engineering, University of Chile, 8370448 Santiago, Chile

HIGHLIGHTS

- A model to grow scale-free networks with tunable motif distributions.
- A combined operation of preferential attachment and triad motif seeding.
- Networks with adjustable distributions of the local triad motifs.
- Networks with "scale-free", "small-world" and high clustering features.

ARTICLE INFO

Article history:
Received 11 August 2014
Received in revised form 7 November 2014
Available online 11 February 2015

Keywords:
Network motif
Motif seeding
Scale-free network
Small-world network
High clustering
Triad motif

ABSTRACT

Network motifs are local structural patterns and elementary functional units of complex networks in real world, which can have significant impacts on the global behavior of these systems. Many models are able to reproduce complex networks mimicking a series of global features of real systems, however the local features such as motifs in real networks have not been well represented. We propose a model to grow scale-free networks with tunable motif distributions through a combined operation of preferential attachment and triad motif seeding steps. Numerical experiments show that the constructed networks have adjustable distributions of the local triad motifs, meanwhile preserving the global features of power-law distributions of node degree, short average path lengths of nodes, and highly clustered structures.

1. Introduction

Complex networks can represent a wide variety of systems in real world, ranging from the Internet to even food webs [1–3]. The elements in these real systems can be described as nodes and their interactions can be seen as links, respectively. Most of these networks share a common group of statistical features: first, they show highly clustered structures compared with random networks; second, the average shortest path between any pair of nodes is relatively small, and this is well known as the "small-world" effect [4]; moreover, the degree of nodes decays as either a power-law distribution [5] or as an exponential distribution [6,7].

To better understand such complex systems, various models have been proposed to describe networks with above three properties over the last decade. Watts and Strogatz introduced a model to represent the small-world networks which have

* Corresponding author.
E-mail address: lisg81@gmail.com (S. Li).

http://dx.doi.org/10.1016/j.physa.2015.02.012
0378-4371/

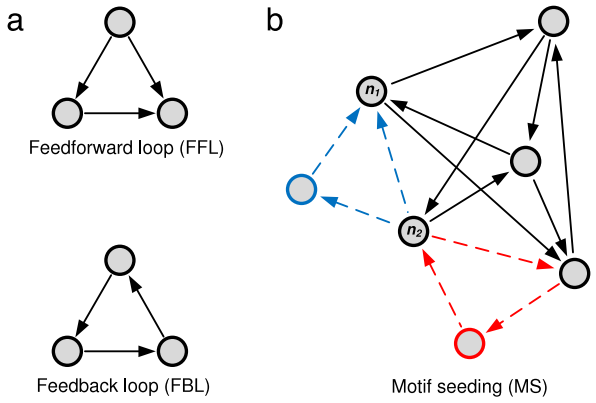

Fig. 1. Motif seeding process. (a) Two looped triad motifs: FFL and FBL. (b) Seeding triad motifs into a network, the blue dashed triangle represents a FFL motif, and the blue circle represents the newly created node; the red dashed triangle is a FBL motif, and the red circle is the newly added node. (For interpretation of the references to color in this figure legend, the reader is referred to the web version of this article.)

small average path lengths as random graphs, and are highly clustered as regular lattices at the same time [4]. Soon later, the scale-free network model was proposed by Barabási and Albert (BA) [5]. This model can characterize networks which have short path lengths and power-law distributions of node degree. However, unlike the small-world networks, the BA model based networks are lack of high clustering in structures. To overcome this limitation, Holme and Kim (HK) modified the BA model by incorporating an additional step called triad formation (TF). As a result, the HK model is able to evolve the networks integrating both scale-free and high clustering features simultaneously [8]. Similarly, Dorogovtsev, et al. also developed a model which can generate clustered scale-free networks through random triad formation steps [9]. Indeed, this simple triangle connection mechanism has also been proven to be the basis for reproducing social networks with short path lengths, high clustering, and scale-free or exponential distributions of node degree [10]. In addition, another model based on a finite memory of nodes has been demonstrated that can induce the growth of highly clustered scale-free networks as well [11].

Although these models show promising results in representing networks of real systems, yet none of them considers the emergence of motifs during structural evolution of networks. Network motifs are frequently appearing small sub-networks consisting of a few nodes and links. They have been discovered across a wide spectrum of networks including biological networks, social networks, electronic circuits, and the World Wide Web, etc. It is generally believed that these motifs serve as basic building blocks of many real world networks [12,13]. A network motif can be understood as a unit which performs a particular information-processing task, or a pattern of a group of specific interacting elements in the system. Moreover, a previous study also reveals that various networks might share very similar distributions of specific motifs, thus the statistical properties of motifs play an essential role in understanding the global structures and functionalities of complex networks [14].

In this paper, we propose a model which can reproduce networks with the properties of high clustering, small average path length, and power law degree distribution, while preserving specific motifs with tunable distributions. This is the first model that simultaneously considers the global structural features of entire networks as well as the distributions of local sub-networks. We should note that our model currently focuses on directed networks, and the mutual connections are forbidden in these networks. Furthermore, a pair of typical triad motifs, the feedforward loop (FFL) and the feedback loop (FBL) as shown in Fig. 1, can be seeded into the structures of networks during their growth processes. Considering the complexity of the seeding process, we currently propose the model only for these unidirectional triad motifs, and a more complete model will be developed in our future work.

2. Motif seeding model

We then introduce this dynamical model by the following growth rules:

1. Initial condition: The initial network has N_0 nodes and L_0 random connections based on the classic Erdös–Rényi (ER) model [15], and the directions of connections are arbitrary but not reciprocal.
2. Growth: At each time step, a new node is created.
3. Motif seeding (MS): In every MS operation, a new node is connected to other two already existing nodes, and the directions of these links are determined by the selected motif pattern. These two existing nodes are chosen by the well-known preferential attachment (PA) operations [16], whereas the selecting probability of each node $P(K_i)$ is based on its in-degree K_{i-in} or out-degree K_{i-out} instead of the node's total degree in undirected networks. It should be noted that, these two nodes must have no connection before MS step in order to guarantee a completely desired motif formation. For instance, when seeding a FFL motif, the node n_1 is selected based on $P(K_{n1})_{in}$, and the other node n_2 is chosen based on $P(K_{n2})_{out}$ as shown in Fig. 1(b). For seeding a FFL motif, each of its 3 possible loops with different links' directions has an equally probability of 1/3 to be seeded by a random rule in this model.

4. Tuning parameters: Including the newly added node, we seed $M(\geq 1)$ motifs into the network. Therefore the number of links increases $3M$ at each time step. As for each MS operation, with probability p, we select the FFL as the formation pattern of a motif; alternatively, a FBL motif will be seeded into network with probability $1 - p$. The growth and MS operations will iterate until the network reaches the given size of N.

As we can learn from above description, the network will be generated entirely by MS steps, which means one node and at least one triad motif consisting of three directed links will be added into network structure at each time step. Therefore, our model can be generally categorized as a TF based model, nevertheless it is quite different from others. First, two independent nodes are chosen by two parallel PA steps in our model, while other models commonly pick a pair of neighbored nodes from the existing network using either PA or randomly choosing operations [8,9,17–19]. More importantly, among all TF based models, our model is the only one that can generate triangle formations using various directed connections.

3. Experiments and results

We verified our model by a series of numerical simulations. The initial conditions were set as $N_0 = 10$, and $L_0 = 22$ (the connection probability is 0.5). The goal sizes of grown networks were fixed to be 40,000 nodes ($N = 40{,}000$) for degree distribution experiments, and 1,000 nodes ($N = 1{,}000$) for other experiments. The main parameters M and p, were varied in different test cases, and the results were averaged over 20 independent trials in each case.

To check the performance of MS operation, the software tool Mfinder (version 1.20) [20] was then used to extract motifs' distributions from the seeded networks. A set of 100 random networks was used for calculating each statistical result of Z-score, and the uniqueness threshold was set as 4 in the Mfinder for detecting triad motifs. Those random networks were generated from the original network using a widely used switching randomization algorithm. This algorithm repeatedly switches the two edges of a randomly chosen connection pair from the original network at each step until the given network is randomized to a target level. Meanwhile, the numbers of in- and out-edge for each node are preserved in this switching process, thus the distributions of in-degree, out-degree, and the total degree are conserved in all randomized networks of the original network [21,12,22]. We should note that the switching algorithm does not make any bidirectional link in the randomization process, since our model prohibits the bidirectional connections in the original networks. As suggested in previous work [14], a motif's statistical significance can be represented quantitatively using the Z-score Z_i and its normalized value Z_i^N as given by Eqs. (1) and (2):

$$Z_i = \frac{(N_{i_{real}} - N_{i_{rand}})}{STD} \tag{1}$$

$$Z_i^N = \frac{Z_i}{\sqrt{\sum Z_i^2}} \tag{2}$$

where $N_{i_{real}}$ is the appearing times of the specific sub-graph i in the original network, and $N_{i_{rand}}$ and STD are the mean and standard deviation of its frequency of appearance in the randomized networks, respectively. The normalized value of Z-score emphasizes the relative significance of a motif over the full spectrum, thus we use it for comparisons in the following studies. A positive Z-score means the motif appears more frequently in the real network, whereas a negative Z-score indicates the motif is less represented in the real network compared with random networks. This definition apparently means that the higher the Z-score, the higher the appearance frequency of a motif, and vice versa. Fig. 2 shows a whole family of five triad motifs' normalized Z-scores under the same seeding frequency $M = 1$ but with different values of the parameter p, while the latter one denotes the seeding probability of the FFL motif.

Interestingly, it is confirmed that these triad motifs' distributions in target networks can be easily controlled through tuning the parameter p. The bar graph demonstrates that the Z-scores of all five types of motifs are significantly varied over a relatively wide range as p changes. For example, along with the rise of p from 0 to 1, the FFL's Z-score steadily increases from 0.03 to 0.52 on average; in contrast, the FBL's Z-score decreases gradually from 0.83 to 0.12 at the same time. Additionally, other three motifs also exhibit different negative Z-scores under various levels of p.

Furthermore, as we can see from the bar graph (Fig. 2), the two looped triad motifs, FFL and FBL both keep positive Z-scores. However the binary-tree motif (BT), the three-chain motif (TC), and the reverse binary-tree motif (RBT) always show negative values on their Z-scores, which means they are underrepresented in the seeded networks, therefore the BT, TC and RBT motifs can be considered as anti-motifs of the seeded networks. We believe this phenomenon might be due to the statistical bias on motifs' appearances, because once a looped motif is counted, then any of its sub-motifs will be no longer considered as an independent one from the looped structure [23,24]. More specifically, a FFL motif has three triad sub-motifs including BT, TC and RBT motifs, while the TC motif is the only one triad sub-motif of a FBL motif. It is easy to understand the relations between these looped motifs and their sub-motifs. The BT, TC and RBT motifs can be obtained if one of these three edges is removed from a FFL motif, similarly we can get a TC motif by deleting one edge from a FBL motif. Consistent with this hypothesis, it is observed that the BT and RBT motifs have exactly the same distributions, and indeed their Z-scores' profiles are both extremely similar to the FFL's distribution but with negative values as its shadow under the $Z = 0$ axis (Fig. 2). We should note that TC shows a more complicated Z-score distribution than BT and RBT, since it serves as sub-motif for both FFL and FBL at the same time.

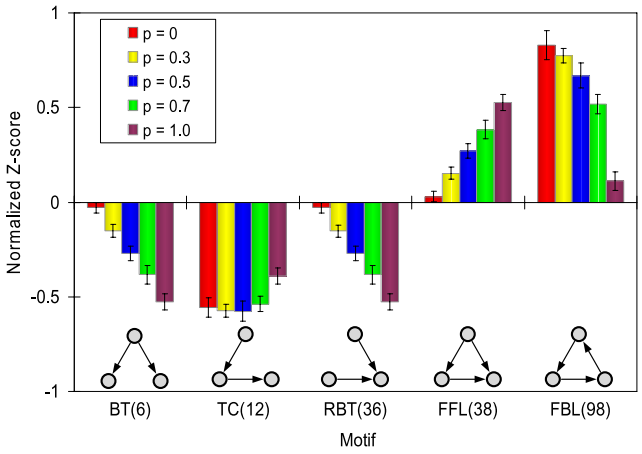

Fig. 2. Triad motifs' distributions in seeded networks. All 5 patterns of triad motifs are shown along the horizontal axis from left to right as the binary-tree (BT, ID: 6), the three-chain (TC, ID: 12), the reverse binary-tree (RBT, ID: 36), the feedforward loop (FFL, ID: 38) and the feedback loop (FBL, ID: 98), respectively. For each pattern of motif, the bars with different colors represent the normalized Z-scores under the same seeding frequency $M = 1$ but using various seeding probabilities p. In particular, the bar with a color of red, yellow, blue, green and grape denotes the case of p equals 0, 0.3, 0.5, 0.7 and 1, respectively. (For interpretation of the references to color in this figure legend, the reader is referred to the web version of this article.)

Table 1
Z-score changes under different M. $Z_{FFL,p=0}$ and $Z_{FFL,p=1}$ indicate the normalized Z-score of FFL motif when $p = 0$ and $p = 1$. Similarly, $Z_{FBL,p=0}$ and $Z_{FBL,p=1}$ represent FBL motif's Z-score (normalized) in the cases of $p = 0$ and $p = 1$.

	$M = 1$	$M = 2$	$M = 3$
$Z_{FFL,p=0}/Z_{FFL,p=1}$	0.03/0.52	0.09/0.51	0.23/0.51
$Z_{FBL,p=0}/Z_{FBL,p=1}$	0.83/0.12	0.81/0.18	0.74/0.22

In addition, there exists a side-effect by which some unexpected FBL motifs emerge during supervised FFL motif seeding process, and vice versa. The side-effect in the former process seems stronger than that in the latter one, which further causes the FBL motifs to appear more frequently than designed in most seeding scenarios. For example, the FBL motif shows a much higher Z-score than the FFL motif at $p = 0.5$ in Fig. 2. This interesting difference of side-effects between two processes is likely to be induced by the topological relations among motifs and their sub-motifs. In particular the FBL motif has higher probabilities to be formed compared to the FFL motif, since it only needs sole sub-motifs of TC.

Next, we investigated how the seeding frequency M influences the features of the seeded networks. The number of edges of the network approached about $3N$, $6N$, and $9N$ ($N = 1{,}000$) after completing the seeding processes, while M was set as 1, 2, and 3, respectively. Interestingly, the normalized Z-score of the FFL motif at $p = 0$ has been significantly increased from 0.03 to 0.23, an almost 8 times' increase, while the FBL motif's Z-score at $p = 1$ was raised from 0.12 to 0.22 for M ranging from 1 to 3 as we can see from Table 1. These changes reveal that the side-effects of motif seeding become stronger when the seeding frequency M increases. We should note that the statistical results of triad motifs shown here might not be accurate enough, as these might include fluctuations and artifacts induced by the switching randomization method in some cases [25,26]. The refined results will be studied in our future work, especially for analyzing the seeded networks with modular or hierarchical structures.

Since our networks consist of many directed motif loops, they are characterized by the in-degree distribution and the out-degree distribution. In Fig. 3(a), we show the in-degree distribution $P_{in}(k)$ and the out-degree distribution $P_{out}(k)$ respectively based on the numerical simulations when $p = 0.5$ and $M = 1$. These two degree distributions of the grown networks have extremely similar curves, therefore we use just the in-degree distributions for our studies hereinafter. Moreover, it is confirmed that the seeding probability p has no significant effect on the networks' degree distributions as presented in Fig. 3(a) inset. As for the networks seeded by different M, their degree distributions all decay following the same power-law denoted as $P(k) \sim k^{-2.3}(\alpha = -2.3)$ as shown in Fig. 3(b). The exponent is different to one from the standard BA model. According to the previous work [27], we believe this may be due to the addition of a new internal edge between two existing nodes at each seeding step compared to the standard BA model. Based on the continuum theory, we can write the change rate of the node degrees in the following form

$$\frac{\partial k_i}{\partial t} = \frac{k_i(t)}{\int_0^t k_j(t)\mathrm{d}t_j} + 2c\frac{k_i(t)\left[\int_0^t k_j(t)\mathrm{d}t_j - k_i(t)\right]}{\left[\int_0^t k_j(t)\mathrm{d}t_j\right]^2 - \int_0^t k_j^2(t)\mathrm{d}t_j} \tag{3}$$

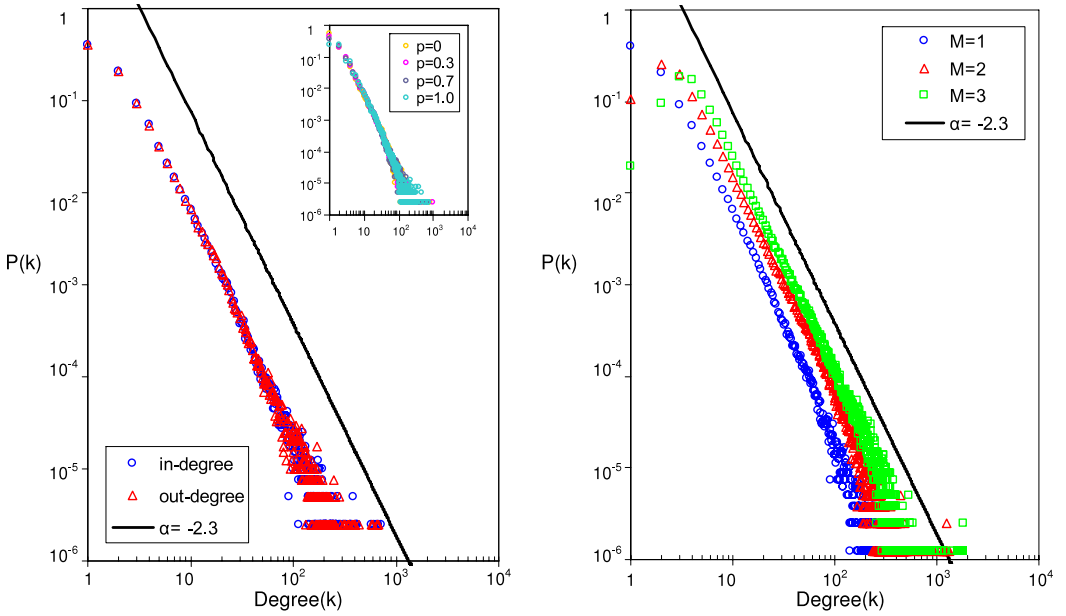

Fig. 3. Degree distributions of seeded networks. (a) Comparison of in/out degrees when $p = 0.5$ and $M = 1$, where the blue circles denote the in-degree distributions and the red triangles represent the out-degree distributions. These two probabilities both decay with the increase of node degree k following a power-law, which has an exponent of $\alpha = -2.3$ (black line). Inset: In-degree distributions under different p when $M = 1$. (b) The open circles (blue), open triangles (red) and open squares (green) indicate the in-degree distributions in the cases of $M = 1$, 2, and 3, respectively. These in-degree distributions share a common power-law scaling with an exponent of $\alpha = -2.3$ (black line). (For interpretation of the references to color in this figure legend, the reader is referred to the web version of this article.)

where k_i is the node's degree, and k_j is the sum of the degrees of all nodes. The first term on the right-hand side describes the linear preferential attachment as in the BA model, and the second term models the addition of c new internal edges between old nodes. The second term can be simplified at long times by neglecting small elements in both numerator and denominator, and then Eq. (3) becomes

$$\frac{\partial k_i}{\partial t} = (1 + 2c)\frac{k_i(t)}{\int_0^t k_j(t)\mathrm{d}t_j} \tag{4}$$

thus the dynamic exponent can be written as

$$\beta = -\frac{1 + 2c}{2(1 + c)} \tag{5}$$

and then we can obtain the exponent of the degree distribution

$$\alpha = -\left(2 + \frac{1}{1 + 2c}\right). \tag{6}$$

This exponent is about -2.3 in our case, since we add only one internal edge at each motif seeding step ($c = 1$).

High clustering is another natural feature of many real networks. The degree of clustering can be measured by the clustering coefficient. The clustering coefficient of node i in our network is calculated as a ratio of existing links E_i among its k_i neighboring nodes to the number of all possible links of these neighbors, which is defined by Eq. (7). The average clustering coefficient of the whole network is obtained by Eq. (8). To calculate the node's clustering coefficient, networks produced by our model can be treated as undirected here, since there is only one directed link between each pair of nodes. The average clustering coefficient seems to be independent of the seeding probability p of the FFL motif in all cases of M as shown in Fig. 4(a). This result suggests that the distributions of various triad motifs have no obvious effect on the clustering characteristics of a seeded network. More importantly, the average clustering coefficient of our network is always significantly higher than that of a random network with the same size and link density as shown in Table 2 in different cases. This indicates that our seeding method can always construct networks with highly clustered structures under a small M.

$$C_i = \frac{2E_i}{k_i(k_i - 1)} \tag{7}$$

$$C = \frac{\sum C_i}{N}. \tag{8}$$

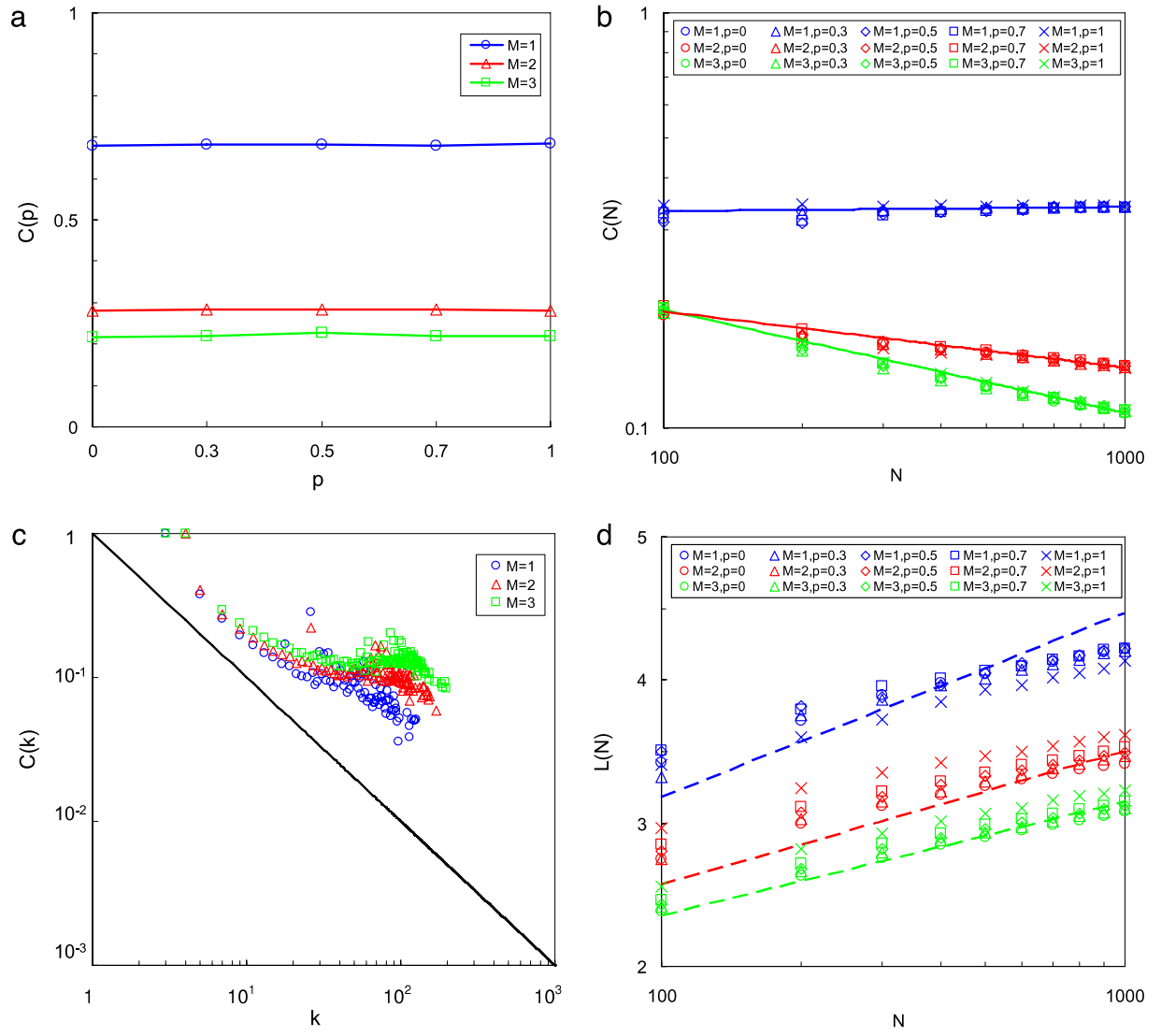

Fig. 4. (a) The dependence of the average clustering coefficient C on the seeding probability p. The open circles (blue), open triangles (red) and open squares (green) correspond to the cases of $M = 1, 2$, and 3. (b) C vs. network size N under different seeding parameters. The blue, red, and green data points represent the cases of $M = 1, 2$, and 3, respectively. The slopes of their fitted lines are 0 (blue), -0.14 (red), and -0.25 (green), respectively. (c) C as a function of the node's in-degree k. The solid line has a slope of -1, while the open circles (blue), open triangles (red) and open squares (green) correspond to $M = 1, 2$, and 3. (d) The scaling law of the average path length L with the network size N under different seeding parameters. The blue, red and green dashed lines represent the average path lengths in the corresponding random networks under different seeding frequencies of M. (For interpretation of the references to color in this figure legend, the reader is referred to the web version of this article.)

Table 2
Comparison of clustering coefficients, where C_{rand} denotes the clustering coefficient of a random network which has the same size of nodes and links as a seeded network.

	$M = 1, L = 3N$	$M = 2, L = 6N$	$M = 3, L = 9N$
C	0.685	0.282	0.220
C_{rand}	0.006	0.012	0.018

Moreover, there is an interesting trend for the seeded networks that the higher the density of seeding, the lower the clustering of grown structures. As shown in Table 2 and Fig. 4(a), the average clustering coefficient decreases as M increases for the seeded networks, however, this trend is completely reversed for their corresponding random networks. This implies that if the seeding frequency M grows to a certain level, this proposed method will not be able to generate highly clustered networks distinguished from random ones. It also provides a way to tune a network with an arbitrary clustering coefficient by altering M during its seeding process.

Fig. 4(b) shows that the average clustering coefficient is nearly independent of the network size N when $M = 1$, whereas it seems to decrease slightly faster when M becomes higher. Furthermore, we find that the relation between the clustering coefficient of a node and the in-degree k approximately follows a power-law $C(k) \sim k^{-1}$ in the case of M equals 1. However, as observed in Fig. 4(c), $C(k)$ becomes more independent of k when M is increased further. This result suggests that our network can be adjusted from a hierarchical structure to a non-hierarchical one [28,29].

To investigate the small-world behavior of the seeded networks, we studied the scaling law of the average path length L with the network size N under different M and p as Fig. 4(d) presents. In general, the data clearly demonstrate that L grows logarithmically with the network size N. These numerical simulations also reveal that our seeded networks have relatively small values of L, which are very close to those values in their corresponding random networks. Therefore, our model is capable of constructing networks with "small-world" features. Moreover, it is found that a higher seeding frequency M seems to reproduce a network with smaller L, while the parameter p affects L slightly once M is fixed.

4. Conclusion

In conclusion, we have presented a motif seeding model for the construction of networks which uniquely reproduces the natural characteristics of real systems. These characteristics describe not only the global structures, such as "scale-free", "small-world" and high clustering, but also the local organizations of various triad motifs. The proposed model simply incorporates a triad-motif seeding action in the preferential attachment process for growing the target network structure. By adjusting only two parameters, the seeding frequency and the seeding probability of the feedforward loop, the network's motif distribution can be continuously varied over a wide range. Meanwhile, numerical simulations also demonstrate that the power-law scaling of degree distribution, the average path length, the clustering coefficient and even the hierarchical structure of the network can be significantly tuned by using proper values of the seeding frequency at each growth step. This study might offer a bottom-up perspective for understanding how the structures and the functionalities of a complex network [30] are simultaneously evolved from scratch. Combined with some network optimization methods [31–33], this study also opens the door to constructing functional networks with desired global behaviors.

Acknowledgment

We thank Professor Hod Lipson of Cornell University for his valuable suggestions and inspirations.

Appendix A. Supplementary data

Supplementary material related to this article can be found online at http://dx.doi.org/10.1016/j.physa.2015.02.012.

References

[1] R. Albert, A.-L. Barabási, Statistical mechanics of complex networks, Rev. Modern Phys. 74 (2002) 47–97. http://dx.doi.org/10.1103/RevModPhys.74.47.
[2] S.N. Dorogovtsev, J.F. Mendes, Evolution of networks, Adv. Phys. 51 (4) (2002) 1079–1187. http://dx.doi.org/10.1080/00018730110112519.
[3] M.E.J. Newman, The structure and function of complex networks, SIAM Rev. 45 (2) (2003) 167–256. http://dx.doi.org/10.1137/S003614450342480.
[4] D.J. Watts, S.H. Strogatz, Collective dynamics of 'small-world' networks, Nature 393 (1998) 440–442. http://dx.doi.org/10.1038/30918.
[5] A.-L. Barabási, R. Albert, Emergence of scaling in random networks, Science 286 (5439) (1999) 509–512. http://dx.doi.org/10.1126/science.286.5439.509.
[6] R. Albert, A.-L. Barabási, Topology of evolving networks: local events and universality, Phys. Rev. Lett. 85 (2000) 5234–5237. http://dx.doi.org/10.1103/PhysRevLett.85.5234.
[7] M.E.J. Newman, The structure of scientific collaboration networks, Proc. Natl. Acad. Sci. USA 98 (2) (2001) 404–409. http://dx.doi.org/10.1073/pnas.98.2.404.
[8] P. Holme, B.J. Kim, Growing scale-free networks with tunable clustering, Phys. Rev. E 65 (2002) 026107. http://dx.doi.org/10.1103/PhysRevE.65.026107.
[9] S.N. Dorogovtsev, J.F.F. Mendes, A.N. Samukhin, Size-dependent degree distribution of a scale-free growing network, Phys. Rev. E 63 (2001) 062101. http://dx.doi.org/10.1103/PhysRevE.63.062101.
[10] J. Davidsen, H. Ebel, S. Bornholdt, Emergence of a small world from local interactions: modeling acquaintance networks, Phys. Rev. Lett. 88 (2002) 128701. http://dx.doi.org/10.1103/PhysRevLett.88.128701.
[11] K. Klemm, V.M. Eguíluz, Highly clustered scale-free networks, Phys. Rev. E 65 (2002) 036123. http://dx.doi.org/10.1103/PhysRevE.65.036123.
[12] R. Milo, S. Shen-Orr, S. Itzkovitz, N. Kashtan, D. Chklovskii, U. Alon, Network motifs: simple building blocks of complex networks, Science 298 (5594) (2002) 824–827. http://dx.doi.org/10.1126/science.298.5594.824.
[13] V.P. Zhigulin, Dynamical motifs: building blocks of complex dynamics in sparsely connected random networks, Phys. Rev. Lett. 92 (2004) 238701. http://dx.doi.org/10.1103/PhysRevLett.92.238701.
[14] R. Milo, S. Itzkovitz, N. Kashtan, R. Levitt, S. Shen-Orr, I. Ayzenshtat, M. Sheffer, U. Alon, Superfamilies of evolved and designed networks, Science 303 (5663) (2004) 1538–1542. http://dx.doi.org/10.1126/science.1089167.
[15] P. Erdös, A. Rényi, On the evolution of random graphs, Publ. Math. Inst. Hung. Acad. Sci. 5 (1960) 17.
[16] A.-L. Barabási, R. Albert, H. Jeong, Mean-field theory for scale-free random networks, Physica A 272 (1) (1999) 173–187. http://dx.doi.org/10.1016/S0378-4371(99)00291-5.
[17] G. Szabó, M. Alava, J. Kertész, Structural transitions in scale-free networks, Phys. Rev. E 67 (2003) 056102. http://dx.doi.org/10.1103/PhysRevE.67.056102.
[18] M. Ángeles Serrano, M. Boguñá, Tuning clustering in random networks with arbitrary degree distributions, Phys. Rev. E 72 (2005) 036133. http://dx.doi.org/10.1103/PhysRevE.72.036133.
[19] Z. Zhang, L. Rong, B. Wang, S. Zhou, J. Guan, Local-world evolving networks with tunable clustering, Physica A 380 (2007) 639–650. http://dx.doi.org/10.1016/j.physa.2007.02.045.

[20] Mfinder:network motifs detection tool, http://www.weizmann.ac.il/mcb/UriAlon/groupNetworkMotifSW.html.
[21] A.R. Rao, R. Jana, S. Bandyopadhyay, A markov chain monte carlo method for generating random (0, 1)-matrices with given marginals, Sankhyā A (1996) 225–242.
[22] R. Milo, N. Kashtan, S. Itzkovitz, M.E.J. Newman, U. Alon, On the uniform generation of random graphs with prescribed degree sequences, arXiv preprint cond-mat/0312028.
[23] A. Vázquez, R. Dobrin, D. Sergi, J.-P. Eckmann, Z.N. Oltvai, A.-L. Barabási, The topological relationship between the large-scale attributes and local interaction patterns of complex networks, Proc. Natl. Acad. Sci. USA 101 (52) (2004) 17940–17945. http://dx.doi.org/10.1073/pnas.0406024101.
[24] S. Li, J. Yuan, J.C. Zagal, Encouraging networks modularity by seeding motifs, in: Proceedings of the 2011 European Conference on Artificial Life, 2011, p. 455.
[25] M.E. Beber, C. Fretter, S. Jain, N. Sonnenschein, M. Müller-Hannemann, M.T. Hütt, Artefacts in statistical analyses of network motifs: general framework and application to metabolic networks, J. R. Soc. Interface 9 (2012) 3426–3435. http://dx.doi.org/10.1098/rsif.2012.0490.
[26] C. Fretter, M. Müller-Hannemann, M.T. Hütt, Subgraph fluctuations in random graphs, Phys. Rev. E 85 (2012) 056119. http://dx.doi.org/10.1103/PhysRevE.85.056119.
[27] S.N. Dorogovtsev, J.F.F. Mendes, Scaling behaviour of developing and decaying networks, Europhys. Lett. 52 (2000) 33. http://dx.doi.org/10.1209/epl/i2000-00400-0.
[28] E. Ravasz, A.L. Somera, D.A. Mongru, Z.N. Oltvai, A.-L. Barabási, Hierarchical organization of modularity in metabolic networks, Science 297 (5586) (2002) 1551–1555. http://dx.doi.org/10.1126/science.1073374.
[29] E. Ravasz, A.-L. Barabási, Hierarchical organization in complex networks, Phys. Rev. E 67 (2003) 026112. http://dx.doi.org/10.1103/PhysRevE.67.026112.
[30] C.H. Comin, M.P. Viana, L.d.F. Costa, The relationship between structure and function in locally observed complex networks, New J. Phys. 15 (2013) 013048. http://dx.doi.org/10.1088/1367-2630/15/1/013048.
[31] T.E. Gorochowski, M. di Bernardo, C.S. Grierson, Evolving enhanced topologies for the synchronization of dynamical complex networks, Phys. Rev. E 81 (2010) 056212. http://dx.doi.org/10.1103/PhysRevE.81.056212.
[32] P. Kaluza, A.S. Mikhailov, Design of robust flow processing networks with time-programmed responses, Eur. Phys. J. B 85 (2012) 129. http://dx.doi.org/10.1140/epjb/e2012-20433-8.
[33] Z. Levnajić, Evolutionary design of non-frustrated networks of phase-repulsive oscillators, Sci. Rep. 2 (2012) 967. http://dx.doi.org/10.1038/srep00967.